EDITORS' CHOICE

Reaction Kinetics of Metal Deposition via Surface Limited Redox Replacement of Underpotentially Deposited Monolayer Studied by Surface Reflectivity and Open Circuit Potential Measurements

Ela Bulut,[a] Dongjun Wu,[a,*] Nikhil Dole,[a] Hasan Kilic,[b] and Stanko R. Brankovic[a,c,,z]**

[a]*Electrical and Computer Engineering Department, University of Houston, Houston, Texas 77204, USA*
[b]*Chemistry Department, Marmara University, Istanbul, Turkey*
[c]*Chemical and Biomolecular Engineering Department, University of Houston, Houston, Texas 77204, USA*

Presented work studies the relation between kinetics of metal deposition via surface limited *redox* replacement (SLRR) of underpotentially deposited (UPD) monolayer (ML) and experimental parameters of reaction solution such as meal ions concentrations and supporting electrolyte concentration. The model system is Au deposition on Au(111) via SLRR of Pb UPD ML. The rate constant of the SLRR reaction for different solution designs is determined from temporal change of electrode surface reflectivity and from the open circuit potential transients' analysis. The obtained results show clearly that reaction kinetics of metal deposition via SLRR of UPD ML is significantly affected by the design of the reaction solution i.e. the UPD metal ion, depositing metal ion, and supporting electrolyte concentrations. The ten-fold change of concentration of either solution parameter produces approximately the same change in the value of the rate constants. The presented results have fundamental importance for the future development and application of the metal deposition via SLRR of UPD ML. They offer a link between the reaction solution design and expected trend in SLRR reaction rate, which transposes to successful control of deposition flux, nucleation density and resulting morphology of the deposit.

 [DOI: 10.1149/2.0471704jes]

Manuscript received January 10, 2017. Published January 28, 2017.

Deposition via Surface Limited Redox Replacement (SLRR) of underpotentially deposited (UPD) monolayer (ML)[1] has gained a lot of attention and applications in last two decades.[2–4] The main idea is to use an UPD ML as sacrificial material to reduce/deposit a more noble metal (SLRR reaction i.e. galvanic displacement). The basic stoichiometry of the SLRR reaction and deposition process is shown by Equation 1.[5]

$$M^0_{UPD}/S(h,k,l)+\left(\frac{m}{p}\right)P^{p+}_{solv} \Rightarrow M^{m+}_{solv}+\left(\frac{m}{p}\right)P^0_s/S(h,k,l) \quad [1]$$

Here, M and P and S(h,k,l) stand for UPD metal/ion, depositing metal/ion and substrate, while m^+/m and p^+/p represent the oxidation state of M and P metal ions and corresponding stoichiometry coefficients. Over the years, several experimental protocols for deposition via SLRR of UPD ML have been developed. The first and the basic one,[1,6] involves formation of the UPD ML of M on the substrate S(h,k,l), (potential controlled step) and then subsequent immersion of M_{UPD}/S(h,k,l) into a separate reaction solution where SLRR occurs and deposition of P takes place at open circuit (sample shuffling approach). The second protocol involves the stagnant substrate but sequential application of potential control in solution for UPD ML formation and then application of solution for SLRR reaction and deposition of P at open circuit (solution shuffling approach[7]). The most recent development has introduced a "*one-solution, one-cell*" experimental design.[8,9] In this case, the same solution serves for UPD ML formation and subsequent SLRR reaction at open circuit potential. This protocol assumes a sequence of potential controlled step, where co-deposition of UPD ML of M with small amount of P occurs, and the open circuit step, where SLRR reaction and deposition of P proceeds. The very details of these three protocols and their applications have been discussed elsewhere in the literature.[4,5,10] Still, more work is necessary to unravel the controlling phenomena of this deposition method and to properly define optimum conditions at which the true benefits of this method are fully exploited.

In many applications concerned with deposition of only a single monolayer of P or ultra-thin films such as core-shell catalyst synthesis for example[2,3,6] (P = Pt, Pd), the properties of deposited films are strong function of their morphology (2D vs. 3D nucleation, cluster size, coverage).[11–16] On the other hand, the morphology of P deposit is a direct function of SLRR reaction kinetics and stoichiometry.[12,17] They are dependent on experimental conditions. These include nature of supporting electrolyte in reaction solution, concentration and oxidation state of the metal ions, complexation and temperature.[5,17,18] Therefore, identifying the fundamental relation between the experimental conditions and resulting kinetics of SLRR reaction should help practitioners to exercise a full control over deposit morphology. This will open new applications of this method in broad spectrum of scales from laboratory experiments to industrial synthesis of core-shell catalysts or wafer level ultrathin thin film growth technologies.[3,4,6,19]

Presented work studies the relation between kinetics of metal deposition via SLRR of UPD ML and experimental parameters of the SLRR reaction. The focus is to evaluate the fundamental effects of concentration of: a) UPD metal ions, b) depositing metal ions, and c) supporting electrolyte, on SLRR reaction kinetics. The model system is Au deposition on Au(111) via SLRR of Pb UPD ML. The experimental protocol in our studies involves "*one solution-one cell*" experimental design where reaction solution contains both Pb^{2+} and Au^{3+} ions and $HClO_4$ as supporting electrolyte.[8] The Pb UPD ML coverage during SLRR reaction is determined from temporal change of electrode surface reflectivity and from analysis of the open circuit potential (OCP) transients.[18,20] Experimental results are fitted with the rate equations for the first order reaction kinetics in terms of Pb UPD ML coverage which is modified to take into account contribution of the oxygen reduction reaction (ORR) occurring in parallel to Au deposition. Our results suggest the existence of proportional and linear trend between the SLRR reaction rate constant and Au^{3+} and Pb^{2+} ion concentrations. We also found that the SLRR reaction rate decreases as the concentration of supporting electrolyte is increased. This study shows that effective manipulation of SLRR reaction kinetics can be achieved by proper design of SLRR reaction solution.

Experimental

General details.—Before each deposition experiment, the starting Au(111) surface (Monocrystals Company) was prepared using mechanical polishing, electropolishing and hydrogen flame annealing. This routinely yielded a highly reflective mirror-like surface finish with very reproducible Pb UPD voltammetry (Figure 3A). All

*Electrochemical Society Student Member.
**Electrochemical Society Member.
[z]E-mail: SRBrankovic@uh.edu

Table I. Range of investigated concentrations.

Ion / support. electrolyte	Au^{3+}	Pb^{2+}	$HClO_4$
Concentration / M	4.4×10^{-5} – 2.6×10^{-4}	10^{-3} – 10^{-2}	0.04 – 0.21

solutions for SLRR reaction were prepared with high purity grade chemicals such as PbO, $HClO_4$ and $AuCl_3$ (99.999%, Alfa Aaeser, Merck) and >18.2 MΩ ultra-pure water (Millipore Direct Q-UV with Barnstead A1007 pre-distillation unit). Before each experiment, solutions are de-aerated for at least one hour with ultrapure nitrogen in order to minimize the concentration of dissolved oxygen from air. All experiments are performed using ultraclean glassware. The volume of spectro-electrochemical cell was 0.150 dm^{-3} while the amount/volume of the reaction solution was standardized to 0.1 dm^{-3} for each experiment. The range of investigated metal ions and supporting electrolyte concentrations are shown in Table I. All potentials in the text are presented as the value of Pb underpotential, ΔE. Fitting of the analytical models to the experimental data (OCP and θ transients) was performed using numerical recipe based on minimization of the residuals' function $\ln(\sqrt{1+R(x)^2})$ to provide the most robust fitting of the data in non-linear regime.[21] The range of the error bars for rate constants is reported as ± the standard deviation of the model fits to experimental data.

SLRR reactions and experimental routine.—The simplified stoichiometry of Au deposition via SLRR of Pb UPD ML from reaction solutions described in Table I is shown by Equation 2;

$$Pb^0_{UPD}/Au(111) + \left(\frac{2}{3}\right) Au^{3+}_{solv} \Rightarrow Pb^{2+}_{solv} + \left(\frac{2}{3}\right) Au^0_s/Au(111) \quad [2]$$

Despite the de-aeration process, the reaction solution inevitably contains some amount of dissolved oxygen. The Pb UPD ML is stable on Au surface at potentials that are significantly more negative than reversible potential for oxygen reduction reaction (ORR). Earlier studies showed that ORR on Pb UPD ML modified electrodes has very fast kinetics.[20,22] At open circuit conditions, where Au deposition occurs via SLRR of Pb UPD ML, dissolved oxygen represents an active specie that can oxidize Pb UPD adatoms and thus competes with Au deposition process. Therefore, SLRR of Pb UPD via dissolved oxygen is the second reaction which has to be taken into account when considering the overall kinetics of Au deposition:

$$Pb^0_{UPD}/Au(111) + \frac{1}{2} O_{2_{solv}} + 2H^+ \Rightarrow Pb^{2+}_{solv} + H_2O \quad [3]$$

For each measurement, our experimental routine followed a sequence of several steps that are illustrated in Figure 1.

In the first step, starting solution contains particular concentrations of Pb^{2+} ions and supporting electrolyte only. This is a potential controlled step in which a cyclic voltammogram is performed to verify the quality of Au(111) surface, and to identify the value of surface reflectivity for Au(111) (θ = 0) and Pb_{UPD}/Au(111) (θ = 1) surfaces. The sweep rate of 0.01 Vs^{-1} in the limits of 0.4 V and 0.005 V ΔE was used.

The second step involves potential pulse from 0.4 V ΔE (no Pb UPD layer on the surface) to 0.005 V ΔE where full Pb UPD ML is formed. Optimum pulse duration is determined by studying the stripping charge from Pb UPD ML deposited using different potential pulse times and solution containing the lowest Pb^{2+} concentration in our studies (10^{-3} M), Figure 2A. As evident from presented data, Pb UPD stripping charge becomes constant for pulse times longer than 3 seconds.

Therefore, a 3 seconds potential pulse to ΔE = 0.005 V to form a full Pb UPD layer is used in all our experiments. After the potential pulse is performed, the cell/potential is disconnected (open

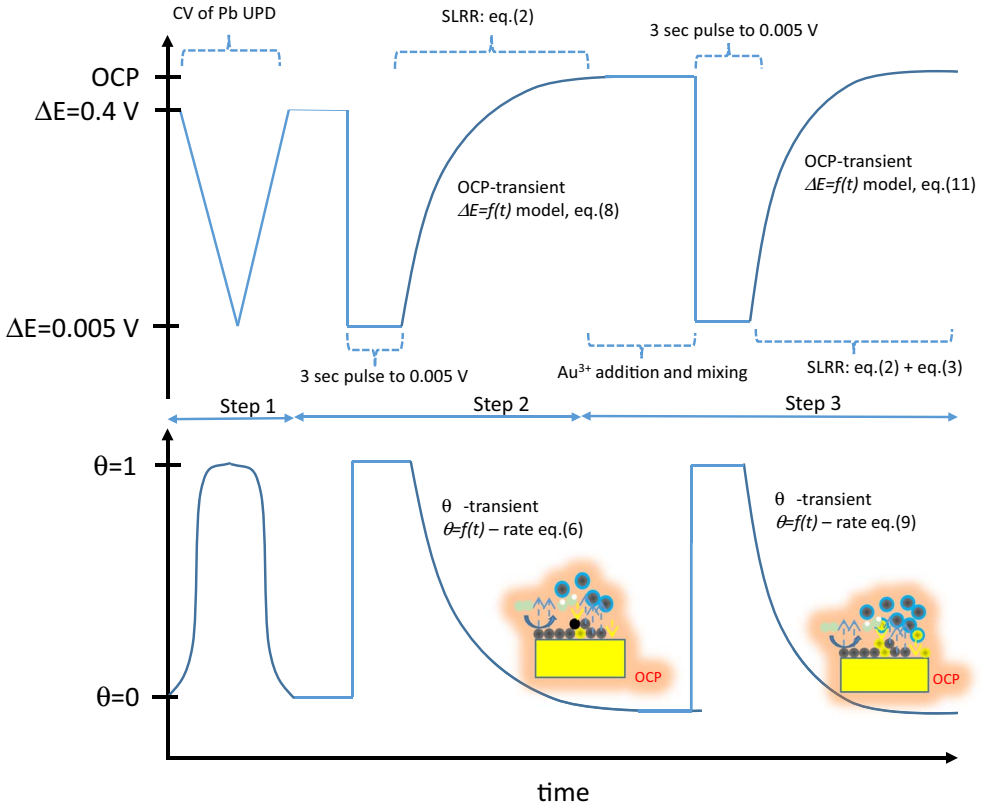

Figure 1. Experimental routine for measurements of reaction rate constants. Each step is marked with corresponding temporal change of potential and Pb UPD coverage.

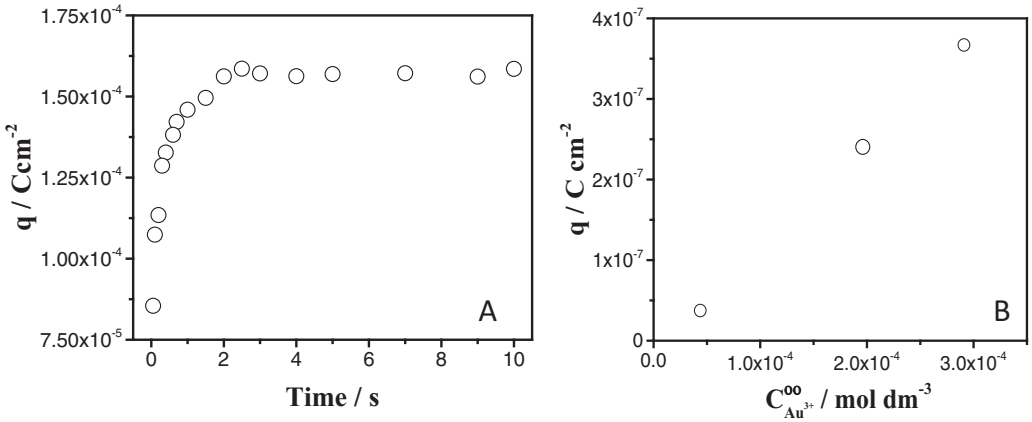

Figure 2. (A) Stripping charge of the Pb UPD ML on Au(111) as a function of the potential pulse duration at $\Delta E = 0.005$ V. Solution: 0.1 M $HClO_4$ + 10^{-3} M Pb^{2+}. (B) Deposition charge during potential pulse from open circuit to 0.005 V ΔE (−0.4 V vs. SCE) for 3 seconds for three different Au^{3+} concentration. Solution: 0.1 M $HClO_4$ + X M Au^{3+}.

circuit potential (OCP) stage, Figure 1) while both, reflectivity/θ and OCP transients, are simultaneously recorded. They are analyzed by appropriate rate equation and OCP model to determine the reaction rate constant for SLRR of Pb UPD ML via dissolved oxygen, Eq. 3, Figure 1.

In the third step, at the beginning, the Au^{3+} containing aliquot (0.003 dm^{-3} of 10^{-3} M Au^{3+}) is added to the starting solution with brief mixing and additional de-aeration for 5 min at OCP, Figure 1. This ensured that desired concentration of Au^{3+} is now present in reaction solution. Then, the potential pulse is performed from OCP to $\Delta E = 0.005$ V for 3 s, and the cell is disconnected, Figure 1. As in previous case, both, potential and reflectivity/θ transients, are simultaneously recorded and analyzed by appropriate rate equation and OCP model to determine now the reaction rate constant for Au deposition via SLRR of Pb UPD ML, Eq. 2, Figure 1. The third step is repeated several more times so that the minimum of three measurements are obtained for particular composition of reaction solution.

It is important to mention that during potential pulse stage in the third step, Figure 1, inevitably some Au co-deposition occurs as well. Because of that, we have performed a detailed measurements to quantify the amount of Au co-deposited and to evaluate if there is a significant change of the electrode surface morphology that could influence the reflectivity data and an overall measurements. The results are shown in Figure 2B. Even in the solution with the highest concentration of Au^{3+} used, < 1/1000 of Au ML is co-deposited with Pb UPD ML ($Q_{Au}^{ML} = 7.2 \times 10^{-4}$ C · cm^{-2}). This is insignificant amount and we assume that Au co-deposition during the Pb UPD ML deposition stage did not affect neither reflectivity nor the rate constant measurements.

Setup for insitu electrode surface reflectivity measurements.— The homebuilt experimental apparatus was used to measure Au electrode reflectivity during Pb UPD and SLRR reactions.[23] It was composed of a CCD camera, a stabilized halogen lamp as the light source, an integrating mirror to collect reflected specular and diffuse light form the electrode surface, the electrochemical cell, data acquisition card (DAQ), connector block, a potentiostat, and several optical bases and holders to allow sturdy fixture of all components to the optical table. An image of the cell and set up are presented in supporting material (S1). ThorLabs DCU223M, black and white, 8-bit CCD camera was used with 1024 × 768 pixel resolution. The CCD camera featured a USB 2.0 connection which allows interfacing for image processing and data acquisition softwares easily. The CCD camera is used in conjunction with Pentax Cosmicar Television lens which had 8.5 mm focal length and 1:1.5 maximum aperture ratio for iris adjustments to prevent pixel saturation.[23] Thorlabs SLS201 stabilized halogen light source was used with fiber optic cable to enable a reproducible light path and incidence angle of 45° to the crystal surface. EG&G Princeton Applied Research 273A Potentiostat provided the current and potential control. It was interfaced with our data acquisition LabVIEW program to achieve temporal recording of current and potential values during the experiments. The LabVIEW program communicated with potentiostat using a multifunction DAQ PCI 6052 E integrated device and NI BNC 2110 connector block. The current and potential acquisition program was also integrated with camera control software. Whenever the voltage and the current are red out and recorded, the LabVIEW data acquisition algorithm triggered the software for capturing an image from CCD camera. This way, the CCD camera is initialized with each potential/current value recorded and an image corresponding to each data point (time, potential, and current) was recorded. The image acquisition and processing software measured the intensity of each recorded image by taking the mean intensity of all pixels in the image array. The maximum speed of image acquisition was 8 images per second. This allowed direct real-time measurements of image intensity vs. time or intensity vs. potential/current.[23]

Insitu image intensity measurements and relation to the surface reflectivity and Pb UPD coverage.—The change in reflectivity of the electrode surface has a linear relationship with intensity change of the reflected light from a surface.[24] In addition to this, it was shown that UPD monolayer coverage has a direct correlation with intensity of the reflected light beam i.e. surface reflectivity.[25–30] This means that the Pb UPD layer coverage (θ) can be obtained from reflectivity measurements using following relation;[25,26]

$$\theta = \frac{R_{Au} - R(\theta)}{R_{Au} - R_{Pb/Au}} \quad [4]$$

Here, R_{Au} is the reflectivity from the gold surface where Pb UPD coverage is zero, (θ = 0), R(θ) refers to the recorded reflectivity values from the reflected light beam during the experiment, and $R_{Pb/Au}$ represents the reflectivity of Au (111) surface fully covered with Pb UPD ML (θ = 1). The reflectivity values can be obtained by multiplying the image/pixel intensities (I) with a factor corresponding to our camera parameters[24] ($R = I \cdot const$). Since the Eq. 4 represents the ratio between reflectivity values, we can directly use measured intensity values from our camera to calculate Pb UPD ML coverage. In that case, for Pb UPD on Au (111), I represents the corresponding intensity of the reflected light from the electrode surface:

$$\theta = \frac{I_{Au} - I(\theta)}{I_{Au} - I_{Pb/Au}} \quad [5]$$

The optical properties of an electrode surface are also the function of the applied potential.[25,27,28] Therefore, the intensity of the reflected light i.e. pixel intensities of an image depends on the electrode

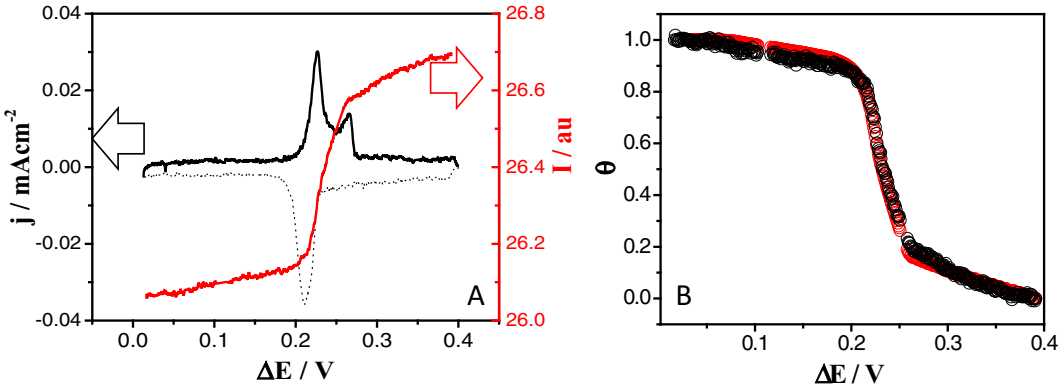

Figure 3. (A) Cyclic voltammogram (CV) for Pb UPD on Au(111). Solution: 5×10^{-3} M Pb^{2+} + 0.1 M $HClO_4$, sweep rate: 0.01 V/s. Sweep in anodic direction is emphasized with solid line for which the corresponding surface reflectivity change is plotted in red. (B) θ vs. ΔE data for Pb UPD on Au(111) reconstructed from (A) using surface reflectivity (red) and charge integration method (black).

potential as well. We have evaluated this effect and found that is comparably very small in the potential range of Pb UPD, i.e. only 2–5% of the total signal change. However, this is taken into account when calculating the Pb UPD ML coverage from the image intensity measurements. The measured intensity values are corrected for the potential dependent change so that the true change of image intensity as a function of Pb UPD coverage is used. The example of Pb UPD coverage (θ) measurements using our insitu reflectivity system is shown in Figure 3A. The reflected light intensity change of the Au (111) surface during anodic sweep in the solution containing 10^{-3} M Pb^{2+} + 0.1 M $HClO_4$ is recorded and corresponding θ is calculated and presented as a function of ΔE (θ - ΔE isotherm from reflectivity data), Figure 3B-red dots. The current-potential data obtained in anodic sweep were also integrated and normalized to obtain the θ-ΔE isotherm from charge integration measurements, Figure 3B-black dots. The comparison of both sets of data shows very good agreement. The relative difference between them is $< 2\%$ which shows that our system is capable of recording the change in θ for the entire UPD potential range, $0 \leq \theta \leq 1$. More importantly, the surface reflectivity measurements are very accurate in recording θ change in $0.1 \leq \theta \leq 0.9$ range which is the most relevant one for our SLRR reaction kinetics studies.

Analytical models for rate equations and fitting of experimental data.—The initial measurements show that the level of dissolved oxygen in reaction solution is of order of $\approx 10^{-6}$ M. This leads to conditions where reaction kinetics of SLRR involving only O_2 and Pb UPD ML, Eq. 3, is controlled by transport, i.e., follows zero order reaction kinetics.[18] Assuming that starting θ is 1, the corresponding rate equation can be written in terms of reaction rate constant, k_0, as.[18,31]

$$\theta = 1 - k_0 t. \qquad [6]$$

As described in our previous work,[18] the k_0 is defined in terms of the surface concentration of Pb UPD monolayer at coverage $\theta = 1$ (Γ_{Pb}^{UPD}), stoichiometry coefficients ratio, $\frac{1}{2}$, bulk concentration of oxygen, $C_{O_2}^{\infty}$, oxygen diffusivity in solution, D_{O_2}, and diffusion layer thickness, δ, Eq. 7;

$$k_0 = \left(\frac{1}{2}\right) \cdot \frac{D_{O_2} \cdot C_{O_2}^{\infty}}{\Gamma_{Pb}^{UPD} \cdot \delta} \qquad [7]$$

The Equation 6 is used to fit θ transients obtained from reflectivity measurements in solutions where no Au^{3+} ions are present and SLRR reaction involves Pb UPD ML oxidation by dissolved O_2, Eq. 3. The OCP transients for this case are fitted by potential-transient model for transport limited *redox* reaction (TLRR) kinetics.[18]

$$E = E_{\theta \to 0} - 0.013\text{V} \cdot \left[\left(\frac{1 - k_0 t}{k_0 t}\right) + f \cdot (1 - k_0 t) + g \cdot (1 - k_0 t)^{3/2}\right] \qquad [8]$$

In the above expression, g, and f stand for *Frumkin*, and *Temkin* energy terms inherited from *Bruckenstein-Swathirajan* (BS) isotherm definition[32] while $E_{\theta \to 0}^{0}$ represents the potential where Pb UPD coverage approaches zero.[18,32] The example of Eq. 6 and Eq. 8 fits of the θ and OCP transients obtained during SLRR of Pb UPD ML by dissolved O_2 are shown in Figure 4.

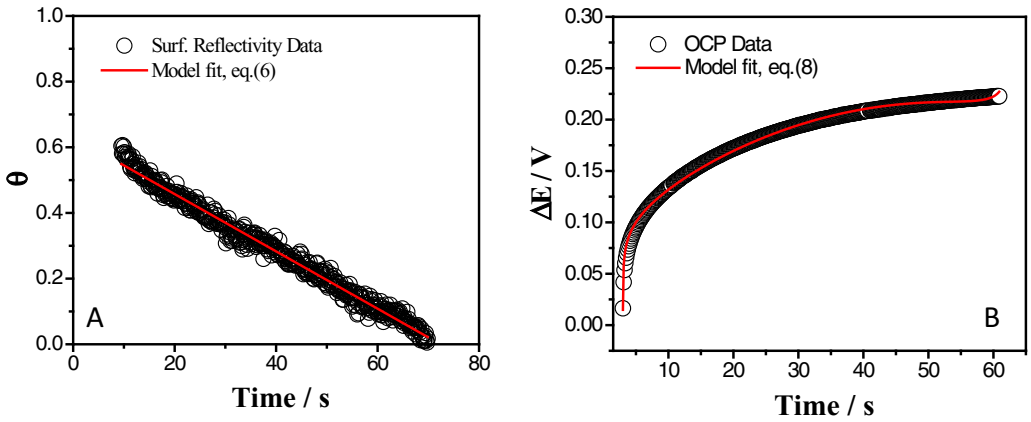

Figure 4. Coverage and OCP transients obtained during SLRR of Pb UPD ML by dissolved O_2. Solution: 0.1 M $HClO_4$ + 10^{-3} M Pb^{2+}. Solution is de-aerated for one hour before measurement. Red line is data fit by Eq. 6 (A) and Eq. 8 (B).

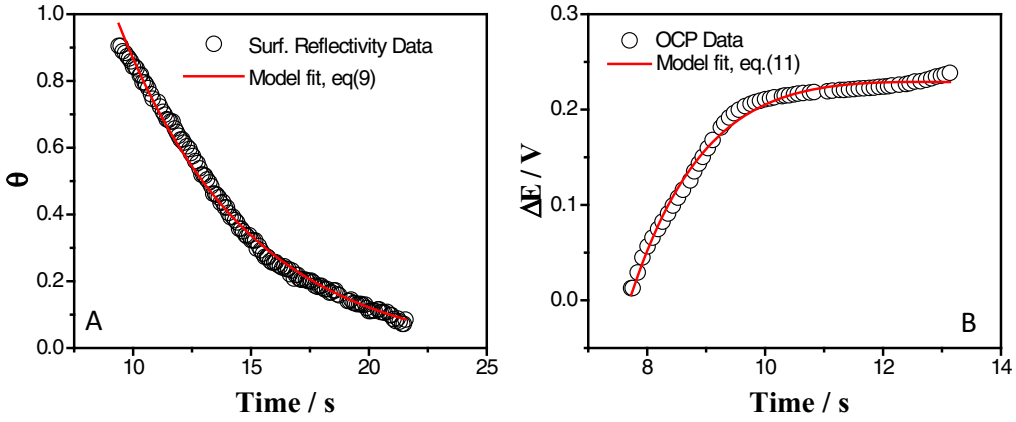

Figure 5. Coverage and OCP transients obtained during Au deposition via SLRR of Pb UPD ML. Solution: 0.1 M $HClO_4$ + 5 × 10^{-3} M Pb^{2+} + 8.5 × 10^{-5} M Au^{3+}. Solution de-aerated for one hour before measurement. Red line is data fit by Eq. 9 (A) and Eq. 11 (B).

When Au^{3+} and dissolved O_2 molecules are present in the solution, both SLRR reactions, Eq. 2 and Eq. 3, occur in parallel. In this case, the best fits of reflectivity and OCP transients are obtained using the rate equation and OCP model which assume the first order reaction kinetics in terms of Pb UPD ML coverage. However, we wanted to eliminate the effect of oxygen on the measurements of reaction rate constant for Au deposition via SLRR of Pb UPD ML. For this reason, we have derived an elaborate form of the first order rate equation which does allow an independent evaluation of the rate constant for Au deposition process, Eq. 2. ("*oxygen-corrected first order rate equation*"). This equation is used for θ and OCP transients' analysis in all deposition experiments. The details of the rate equation and OCP model derivations are presented in the Appendix of the paper. Here, we show only the final form of the equations used for fitting. Therefore, the θ vs. *t* data obtained when both Au^{3+} and O_2 are present in reaction solution are fitted with Eq. 9,

$$\theta(t) = \left(1 + \frac{k_0}{k'}\right) e^{-k't} - \frac{k_0}{k'}. \qquad [9]$$

The term k' represents the rate constant for Au deposition via SLRR of Pb UPD ML. It is defined in terms of the fundamental rate constant, k, surface concentration of Au^{3+}, C_{Au}^{is}, and reaction order in terms of Au^{3+} reactant, L:[18]

$$k' = k\left(C_{Au}^{is}\right)^{L} \quad \left[s^{-1}\right], \qquad [10]$$

The OCP transients obtained during experiments where both, Au^{3+} and O_2, are present in the reaction solution are fitted with model that is derived combining the Eq. 9 with BS isotherm[18,32] (see Appendix), Eq. 11,

$$E = E_{\theta\to 0} - 0.013\text{V}\left\{ ln\frac{\left((1+\frac{k_0}{k'})e^{(-k't)} - \frac{k_0}{k'}\right)}{\left(1+\frac{k_0}{k'} - (1+\frac{k_0}{k'})e^{(-k't)}\right)} + f\left((1+\frac{k_0}{k'})e^{(-k't)} - \frac{k_0}{k'}\right) + g\left((1+\frac{k_0}{k'})e^{(-k't)} - \frac{k_0}{k'}\right)^{3/2}\right\} \qquad [11]$$

The example of Eq. 9 and Eq. 11 fits of the θ and OCP transients obtained during deposition experiments are shown in Figure 5.

Results and Discussion

Au^{3+} concentration effect on reaction kinetics of Au deposition via SLRR of Pb UPD monolayer.—Experiments studying the effect of Au^{3+} concentration (C_{Au}^{∞}) involved its methodical variation in reaction solution and evaluation of the corresponding rate constants while keeping the Pb^{2+} concentration *const*. The measurements with different Au^{3+} concentrations are grouped in a set for each particular concentration of Pb^{2+} in reaction solution. The individual θ and OCP transients during SLRR reaction and models' fits (Eq. 6–Eq. 11) are presented in the supporting material (S2–S9). Here, we show only numerical values of rate constants extracted from these measurements and analysis, Table II and Table III. The summary of results is plotted as k' vs. C_{Au}^{∞} in Figure 6. The composition of the base solution for each set of experiments is indicated in the sub-headers of the Table II and Table III and in Figure 6. Each set represents eight measurements of the rate constants obtained for C_{Au}^{∞}. The investigated values of C_{Au}^{∞} are: 0 M; 4.3 × 10^{-5} M; 8.5×10^{-5} M; 1.2 × 10^{-4} M; 1.6 × 10^{-4} M; 2.0 × 10^{-4} M; 2.3 × 10^{-4} M; and 2.6 × 10^{-4} M. The values of Pb^{2+} concentration start with 10^{-3} M in the 1st set of experiments and increase to 3 × 10^{-3} M, 5 × 10^{-3} M and 10^{-2} M in the 2nd, 3rd and 4th set. For each set, the first experiment involves solution which does not contain any Au^{3+} ions. The θ and OCP transient from this experiment are fitted with Eq. 6 and Eq. 8 to extract the value of k_0 (SLRR reaction defined by Eq. 3). Such determined value of k_0 is then used as fixed parameter in the model represented by Eq. 9 and Eq. 11 to fit θ and OCP transients from particular set of Au deposition experiments. This way, we were able to extract independently the values of the rate constant k' as a function of C_{Au}^{∞} (SLRR reaction defined by Eq. 2). In general, a very good quality of fits is obtained in all experiments which is indicated by small values of standard deviations of the fits, Table II and Table III (see also support material S2–S9).

The extracted rate constants from both, OCP and reflectivity, measurements show qualitative agreement in terms of the observed k' vs. C_{Au}^{∞} trend. The results obtained from surface reflectivity measurements have slightly lower k' values as compared to ones obtained from OCP measurements, Figure 6A vs Figure 6B. The values of k' obtained from OCP measurements show slightly more scattering, and somewhat larger standard deviation of the fits. This is not surprising since the model used to fit OCP transients possess more complexity and fitting parameters. The obtained results suggest that k' vs C_{Au}^{∞} dependence for each set of experiments has linear trend. It shows an increase in k' with increasing C_{Au}^{∞} i.e. more Au^{3+} in solution yields a faster deposition kinetics. The proportional relation between k' and C_{Au}^{∞} observed in both measurements is expected if one considers definition of k', Eq. 10. However, the observed linear trend deserves a closer look. To proceed further, we have to define first the relation between the surface concentration of gold, C_{Au}^{is}, which enters definition of k', and its bulk value which is controlled parameter in the experiments. We expressed the C_{Au}^{is} as a product of the interface width, ξ, and the bulk value of Au^{3+} concentration (C_{Au}^{∞}),[33]

$$C_{Au}^{is} = C_{Au}^{\infty} \cdot \xi \cdot \quad \left[\text{mol}\cdot\text{dm}^{-2}\right] \qquad [12]$$

Table II. The values of rate constants extracted from surface reflectivity measurements for different Au^{3+} concentration. Base solution for each experimental set is indicated in sub-header of the table.

1st Set:		Base Electrolyte: 0.1 M $HClO_4$ + 10^{-3} M Pb^{2+}						
C^{∞}_{Au}/M	0	4.3×10^{-5}	8.5×10^{-5}	1.2×10^{-4}	1.6×10^{-4}	2.0×10^{-4}	2.3×10^{-4}	2.6×10^{-4}
k' *or* k_0 /s^{-1}	0.00873	0.02039	0.08058	0.09296	0.15288	0.19537	0.24296	0.27780
$\pm\sigma$ / s^{-1}	4.76E-5	0.00002	0.00073	0.00099	0.00179	0.00338	0.00230	0.00384
2nd Set		Base Electrolyte: 0.1 M $HClO_4$ + 3×10^{-3} M Pb^{2+}						
C^{∞}_{Au} / M	0	4.3×10^{-5}	8.5×10^{-5}	1.2×10^{-4}	1.6×10^{-4}	2.0×10^{-4}	2.3×10^{-4}	2.6×10^{-4}
k' or k_0 /s^{-1}	0.01690	0.01232	0.05409	0.10597	0.15789	0.23217	0.26798	0.23780
$\pm\sigma$ / s^{-1}	7.12E-5	3.13E-4	0.00070	0.00152	0.00218	0.00860	0.004773	0.00631
3rd Set		Base Electrolyte: 0.1 M $HClO_4$ + 5×10^{-3} M Pb^{2+}						
C^{∞}_{Au}/ M	0	4.3×10^{-5}	8.5×10^{-5}	1.2×10^{-4}	1.6×10^{-4}	2.0×10^{-4}	2.3×10^{-4}	2.6×10^{-4}
k' or k_0 /s^{-1}	0.00467	0.03897	0.09899	0.17997	0.24319	0.29162	0.34231	0.37922
$\pm\sigma$ / s^{-1}	1.45E-4	0.00020	0.00067	0.00152	0.00206	0.00375	0.00363	0.00718
4th Set		Base Electrolyte: 0.1 M $HClO_4$ + 10^{-2} M Pb^{2+}						
C^{∞}_{Au}/ M	0	4.3×10^{-5}	8.5×10^{-5}	1.2×10^{-4}	1.6×10^{-4}	2.0×10^{-4}	2.3×10^{-4}	2.6×10^{-4}
k' or k_0 /s^{-1}	0.00994	0.17487	0.26258	0.34861	0.40956	0.49651	0.57528	0.65082
$\pm\sigma$ / s^{-1}	4.53E-5	0.00235	0.00396	0.00879	0.00727	0.00589	0.01149	0.02062

Table III. The values of rate constants extracted from OCP measurements for different Au^{3+} concentration. Base solution for each experimental set is indicated in sub-header of the table.

1st Set		Base Electrolyte: 0.1 M $HClO_4$ + 10^{-3} M Pb^{2+}						
C^{∞}_{Au} / M	0	4.3×10^{-5}	8.5×10^{-5}	1.2×10^{-4}	1.6×10^{-4}	2.0×10^{-4}	2.3×10^{-4}	2.6×10^{-4}
k' or k_0 /s^{-1}	0.01693	2.35E-6	0.01788	0.00453	0.03440	0.06150	0.02667	2.35E-6
$\pm\sigma$ / s^{-1}	5.07E-5	0.00028	0.00097	0.01037	0.00952	0.01631	0.01687	0.00028
2nd Set		Base Electrolyte: 0.1 M $HClO_4$ + 3×10^{-3} M Pb^{2+}						
C^{∞}_{Au}/ M	0	4.3×10^{-5}	8.5×10^{-5}	1.2×10^{-4}	1.6×10^{-4}	2.0×10^{-4}	2.3×10^{-4}	2.6×10^{-4}
k' or k_0 /s^{-1}	0.06124	0.03147	0.14762	0.34060	0.41915	0.67855	0.58264	0.70710
$\pm\sigma$ / s^{-1}	0.00019	0.00054	0.00189	0.00551	0.03976	0.05377	0.09404	0.10038
3rd Set		Base Electrolyte: 0.1 M $HClO_4$ + 5×10^{-3} M Pb^{2+}						
C^{∞}_{Au} / M	0	4.3×10^{-5}	8.5×10^{-5}	1.2×10^{-4}	1.6×10^{-4}	2.0×10^{-4}	2.3×10^{-4}	2.6×10^{-4}
k' or k_0 /s^{-1}	0.00136	0.17908	0.32837	0.38908	0.53721	0.47640	0.63730	0.56155
$\pm\sigma$ / s^{-1}	0.00657	0.00596	0.02419	0.08484	0.08883	0.23377	0.26553	0.31982
4th Set		Base Electrolyte: 0.1 M $HClO_4$ + 10^{-2} M Pb^{2+}						
C^{∞}_{Au} / M	0	4.3×10^{-5}	8.5×10^{-5}	1.2×10^{-4}	1.6×10^{-4}	2.0×10^{-4}	2.3×10^{-4}	2.6×10^{-4}
k' or k_0 /s^{-1}	0.06589	0.45688	0.55804	0.68049	0.79077	0.74972	1.21496	1.39606
$\pm\sigma$ / s^{-1}	0.69889	0.06277	0.09858	0.13434	0.16876	0.26981	0.32389	0.32728

Therefore, the expression for k' in terms of C^{∞}_{Au} is rewritten as:

$$k' = k\left(C_P^{is}\right)^L = k\left(C^{\infty}_{Au} \cdot \xi\right)^L = k \cdot \xi^L \cdot \left(C^{\infty}_{Au}\right)^L. \qquad [13]$$

Now, with more comprehensive definition of k', the linear trend in our k' vs. C^{∞}_{Au} data in Figure 6 has a real physical meaning. It indicates that the value of L is 1. This means that Au deposition via SLRR of Pb UPD monolayer is the first order in terms of bulk Au^{3+} reactant. This result is expected because the Au deposition via SLRR of Pb UPD ML can be considered as elementary reaction, and stoichiometry coefficients can be taken as the order of reaction in terms of its reactants. From Eq. 2, it is evident that one Au atom reacts with 1.5 Pb UPD atoms,

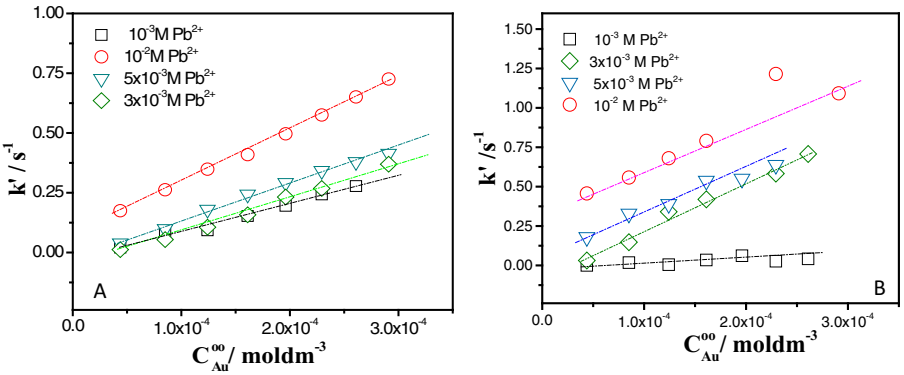

Figure 6. (A) Summary of the rate constant values extracted from surface reflectivity (Table II) and (B) from OCP measurements (Table III).

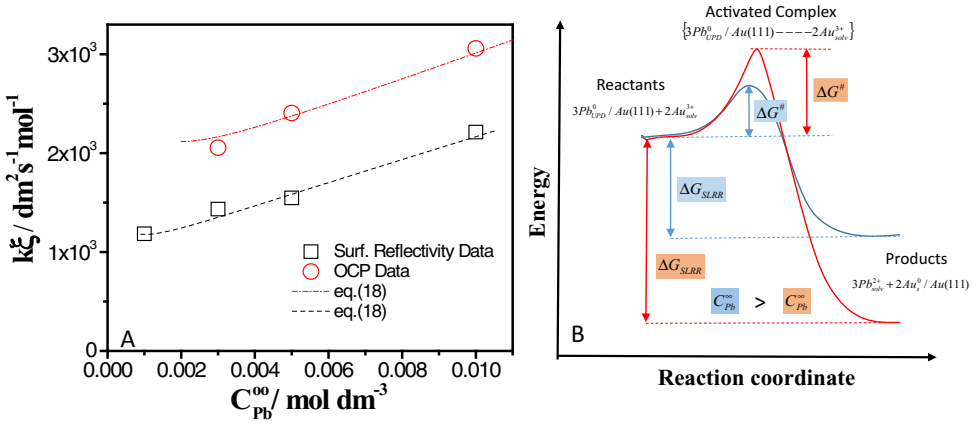

Figure 7. (A) Slope for each set of data in Figure 6 plotted as a function of the Pb^{2+} concentration. Black dots–surface reflectivity (Figure 6A) and red dots-OCP measurements (Figure 6B). Dotted lines represent fits of Eq. 18. (B) Schematics illustrating change of ΔG_{SLRR} and $\Delta G^{\#}$ with increasing C^{∞}_{Pb}.

and $L = 1$ in terms of Au^{3+} can be assumed. Therefore, our results confirm that gold deposition via SLRR of Pb UPD ML represents an elementary *redox* reaction indeed. However, our conclusion should be limited only to the range of C^{∞}_{Au} that were investigated.

If we are to extend our discussion to lower limits of C^{∞}_{Au}, we could expect, at some point, that transport will start to control the Au deposition kinetics. Therefore, further decrease of C^{∞}_{Au} below the 4.3×10^{-5} M may result in reaction order change in terms of Au^{3+} reactant from 1 to 0.[18]

Effect of Pb^{2+} concentration on reaction kinetics of Au deposition via SLRR of Pb UPD monolayer.—One important result which is evident from both types of measurements is that an increase in concentration of Pb^{2+} in reaction solution (C^{∞}_{Pb}) leads to a higher values of k'. A more detailed look of the k' vs. C^{∞}_{Au} dependences also shows that the slope in the k' vs. C^{∞}_{Au} data has a very strong dependence on the C^{∞}_{Pb}. This is shown in Figure 7A. We proceed with further analysis of this observation by having in mind definition of k' presented by Eq. 13. Therefore, we can express the slope for data sets in Figure 6 (for $L = 1$) as;

$$slope = k \cdot \xi^{L} = k\xi. \qquad [14]$$

From both types of measurements a linear dependence is observed between the value of $k \cdot \xi$ and corresponding C^{∞}_{Pb}, which are plotted in Figure 7A ($k \cdot \xi$ vs. C^{∞}_{Pb}). A higher concentration of Pb^{2+} in reaction solution leads to a larger values of $k \cdot \xi$. The $k \cdot \xi$ values from OCP data are shifted upward reflecting in general a slightly higher values of k' obtained from OCP transients analysis shown in Figure 6. However, OCP and surface reflectivity measurements produce almost identical $k \cdot \xi$ vs. C^{∞}_{Pb} dependence. The slopes of both linear trends are identical, Figure 7A. Considering that at given conditions, the ξ can be taken as numerical constant,[33] one concludes that magnitude of C^{∞}_{Pb} has significant effect on the fundamental rate constant for SLRR reaction. The 100% increase in the value of k (or $k\xi$) is observed for one order of magnitude increase in Pb^{2+} concentration. At this point we make a modest effort to derive an approximate phenomenological description of this relation. For this purpose, we recall the basic definition of the fundamental rate constant from transition state theory;[34]

$$k \propto \exp\left(-\frac{\Delta G^{\#}}{k_B T}\right). \qquad [15]$$

Here, $\Delta G^{\#}$ represents the free energy of Pb UPD adatom-Au^{3+} ion activated complex illustrated in Figure 7B. From basic postulates of *Marcus* theory[35] of charge transfer we can adopt the definition of $\Delta G^{\#}$ (*Marcus* inverted region) as:

$$\Delta G^{\#} = \frac{(\Delta G_{SLRR} + \lambda)^2}{4\lambda}. \qquad [16]$$

The ΔG_{SLRR} is the free energy of the SLRR reaction, Figure 7B, and λ is the sum of the inner and outer reorganization energy ($\lambda = \lambda_{in} + \lambda_{out}$).[35] From basic thermodynamic relations we know that ΔG_{SLRR} is directly proportional to the electrochemical driving force for SLRR reaction, ΔE_{SLRR} ($\Delta G_{SLRR} = -(m/p)F\Delta E_{SLRR}$). The exact phenomenological description of ΔE_{SLRR} term have been done in our previous work.[1,5] Recalling this results we can write proportional relation between ΔG_{SLRR} and thermodynamic quantities defining ΔE_{SLRR} as:[5]

$$\Delta G_{SLRR} \propto -\left\{\Delta E^{0}_{EMF} - \Delta E^{0}_{\theta\to 0} - \frac{k_B T}{e} \ln \frac{[a_{M^{m+}}]^m}{[a_{P^{p+}}]^p}\right\} \qquad [17]$$

Here, ΔE^{0}_{EMF} ($\Delta E^{0}_{EMF} = E^{0}_{P^{p+}/P} - E^{0}_{M^{m+}/M}$) represents the electromotive force for the bulk M and P galvanic couple (Pb and Au) at standard conditions. The $\Delta E^{0}_{\theta\to 0}$ is the underpotential for M UPD ML at $\theta \to 0$ limit (Pb UPD shift at $\theta \to 0$ limit) at standard conditions and $a_{M^{m+}}$ and $a_{P^{p+}}$ are activities of the ions in the reaction solution (Pb^{2+} and Au^{3+}).[1,5] The logarithmic term in the above expression provides correction for departure from standard conditions and m and p represent stoichiometry coefficients in the SLRR reaction (Eq. 1 and Eq. 2). Combining Eq. 15–Eq. 17 and assuming the notation for our case where M = Pb and P = Au, and taking $a_{M^{m+}} = a_{Pb^{2+}} \approx C^{\infty}_{Pb}$ and $a_{P^{p+}} = a_{Au^{3+}} \approx C^{\infty}_{Au} = const$ we arrive to the expression which describes the functional relation between the fundamental rate constant k and C^{∞}_{Pb}:

$$k \propto \exp\left(-A - B \cdot \ln(C^{\infty}_{Pb}) - C \cdot (\ln(C^{\infty}_{Pb}))^2\right). \qquad [18]$$

The terms A, B and C represent a physical constants that absorb an intricate relation between fundamental physical constants such as e, k_B, and parameters of the UPD and SLRR system such as ΔE^{0}_{EMF} and $\Delta E^{0}_{\theta\to 0}$ m, p, and λ. The experimental parameters that are set *const* in our analysis such as T and C^{∞}_{Au} are also absorbed into the value of A, B and C constants. The fit of the functional defined by Eq. 18 to $k\xi$ vs. C^{∞}_{Pb} data is plotted in Figure 7A-dashed lines. Obviously, the mathematical form of the Eq. 18 successfully captures the observed trend. Therefore, we conclude that effect of increasing C^{∞}_{Pb} lowers the free energy for SLRR reaction (Eq. 17), which in turn leads to a lower free energy of the activated complex (energy barrier) for SLRR reaction, (Eq. 16). Consequently, this leads to a larger values of fundamental rate constant for SLRR reaction (Eq. 15). This conclusion is illustrated in Figure 7B.

It has to be mentioned here that same qualitative conclusion about effect of C^{∞}_{Pb} on k can be deduced by considering the kinetic theory of reaction rate.[36] Here, we point out that the Pb^{2+} concentration in the electrolyte has a direct relation to the frequency factor entering the definition of the fundamental rate constant k.[36,37] This becomes more transparent if one recalls definition of the exchange current density for

Table IV. Values of rate constants extracted from surface reflectivity measurements for different concentration of supporting electrolyte.

	Base Electrolyte: 10^{-3} M Pb^{2+} + 1.35 × 10^{-4} M Au^{3+}							
$C^{\infty}_{HClO_4}$ / M	0.01	0.04	0.07	0.095	0.12	0.14	0.17	0.2
k' / s^{-1}	0.04913	0.06085	0.05734	0.04769	0.04405	0.03952	0.03074	0.02474
±σ / s^{-1}	0.00140	1.51E-3	0.00162	0.00049	0.00184	0.00166	0.00150	0.00106

Table V. Values of rate constants extracted from OCP measurements for different concentration of supporting electrolyte.

	Base Electrolyte: 10^{-3} M Pb^{2+} + 1.35 × 10^{-4} M Au^{3+}							
$C^{\infty}_{HClO_4}$ / M	0.01	0.04	0.07	0.095	0.12	0.14	0.17	0.2
k' / s^{-1}	NA	0.04506	0.05624	0.05521	0.04679	0.03613	NA	NA
±σ / s^{-1}	NA	0.032872	0.058408	0.040622	0.046579	0.027997	NA	NA

an electrode/metal surface in contact with its ions in solution.[38] The increase in Pb^{2+} concentration leads to a larger rate of dynamic exchange between Pb UPD adatoms and Pb^{2+} ions in the solution.[38,39] Therefore, we should expect that larger Pb^{2+} concentration produces a higher Pb UPD adatom-Au^{3+} collision frequency as well. This is a prelude to higher probability of reactive collision between Pb UPD adatoms and Au^{3+} ions yielding a larger values of fundamental rate constant.

Effect of supporting electrolyte on reaction kinetics of Au deposition via SLRR of Pb UPD monolayer.—In order to study the effect of supporting electrolyte on reaction kinetics we have performed the set of eight measurements in reaction solution containing X M $HClO_4$ + 10^{-3} M Pb^{2+} + 1.35 × 10^{-4} M Au^{3+} (X = 0.01 M; 0.04 M; 0.07 M; 0.095 M; 0.12 M; 0.14 M; 0.17 M; and 0.19 M). The individual Pb UPD coverage and OCP transients together with model fits to extract the rate constant are shown in supporting material (S10-S11). Here we show only numerical values of extracted k', Table IV and Table V and results summary plotted as k' vs. $HClO_4$ concentration (k' vs. $C^{\infty}_{HClO_4}$), Figure 8. The k' values extracted from OCP data have shown significantly larger standard deviations and thus they are less confident. For this reasons, some of the data are excluded from the plot in Figure 8B. Importantly, approximately the same values of k' for given range of investigated $C^{\infty}_{HClO_4}$ were extracted from both types measurements. The data yield a linear regression. The effect of $C^{\infty}_{HClO_4}$ is quite strong and it demonstrates that manipulation with supporting electrolyte concentration is an elegant way to fine tune kinetics of SLRR reaction. In our case, the 300% increase in rate constant is achieved easily by ten-fold dilution of supporting electrolyte.

Analyzing data in Table IV and Table V and Figure 8 one must appreciate the fact that perchlorate ion does not have any complexing ability toward either Pb^{2+} or Au^{3+} ions.[40] Furthermore, it is likely that Au^{3+} is in its chloride complex (solution prepared from $AuCl_3$ salt) as $\{AuCl_4\}^-$ which is much more stable than Au^{3+} complexed with $\{ClO_4\}^-$ ions. In addition to this, for the range of studied $C^{\infty}_{HClO_4}$ one do not expect a major change in the value of ξ and thus it can be considered as $\xi = const$.[33] In addition to that, we keep $C^{\infty}_{Pb} = const$ and $C^{\infty}_{Au} = const$ in these experiments. There is neither obvious effect of supporting electrolyte on reacting species nor there is an obvious relation between its concentration and definition of k' (Eq. 13). However, the observed trend can be explained by considering a basic postulates of *Debye-Huckel* theory of electrolyte.[41] A stronger presence of supporting electrolyte in the solution influences Debye length, λ_D, which is a distance at which the ion charge and coulomb potential are completely screened by surrounding ions in the solution. For symmetric supporting electrolyte such as perchloric acid, *Debye* length has $\lambda_D \infty (C^{\infty}_{HClO_4})^{-0.5}$ dependence. Therefore, more perchlorate ions in solution will reduce the value of *Debye* length. This means that the effective coulomb field surrounding a potentially reacting Au^{3+} ion at the surface is felt at the shorter distance if reaction solution contains more $HClO_4$. Because of that, the distance of the approach between Au^{3+} and Pb UPD adatoms necessary for effective electron transfer/tunneling has to be shorter. This leads to lower spatial probability of reactive encounter between Pb UPD adatoms and Au^{3+} ions and one could expect a slower kinetics of the *redox* process and lower values of the rate constant in solution with higher $C^{\infty}_{HClO_4}$.

Conclusions

Our work successfully demonstrates that surface reflectivity is an enabling method to study the reaction kinetics of metal deposition via SLRR of UPD ML. Evidently, it does possess certain advantages over conventional OCP transients based approach. It offers a direct way to measure the change in UPD ML coverage during SLRR reaction hence allowing results analysis with equations that have less complexity and fitting parameters as compared to the models developed

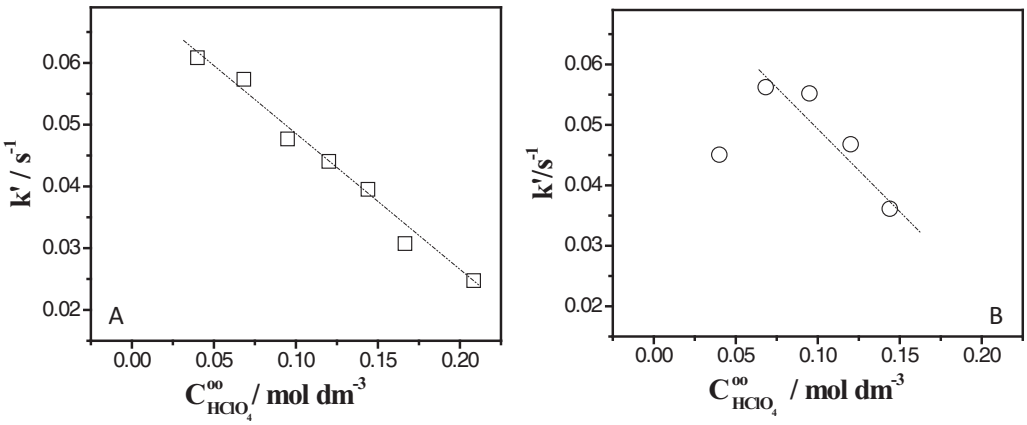

Figure 8. Summary of rate constants values plotted as a function of supporting electrolyte concentration. (A) Data form surface reflectivity, Table IV and (B) from OCP measurements, Table V.

for OCP based kinetics studies.[18] The obtained results show clearly that reaction kinetics of metal deposition via SLRR of UPD ML is significantly affected by the design of the reaction solution i.e. the UPD metal ion, depositing metal ion, and supporting electrolyte concentrations. Importantly, none of these parameters has predominant effect on the reaction kinetics. Our study shows that ten-fold change of concentration of either solution parameter produces approximately the same change in the value of the rate constants. In addition to these findings, our study shows for the first time that UPD metal concentration represents an extra nob to fine tune deposition kinetics. One of the findings that certainly deserves more experimental and theoretical studies in the near future is the effect of supporting electrolyte on reaction kinetics. This, result suggests that proper design of supporting electrolyte concentration in reaction solution is an elegant way to control the speed of SLRR reaction and thus to control the metal deposition rate. We believe that results presented here have fundamental importance for the future development and application of the metal deposition via SLRR of UPD ML. They offer a link between the reaction solution design and expected trend in SLRR reaction rate, which transposes to successful control of deposition flux, nucleation density[12,17] and resulting morphology of the deposit.[4,11]

Acknowledgment

The authors thank Professor Eric Bittner from Chemistry Department, UH for helpful discussions. This material is based upon work supported by the National Science Foundation under the contract CHE-0955922. E. B. and H. K. acknowledge support from Turkish Ministry of Education and The Scientific and Technological Research Council of Turkey.

Appendix

Derivation of "oxygen corrected" first order rate equation.—The change of the Pb UPD layer coverage during Au deposition which takes both SLRR reactions (Eq. 2 and Eq. 3) into account can be presented as the first order linear differential equation with constant coefficients, k' and k_0 (Eq. 7 and Eq. 13). The change in Pb UPD ML coverage is expressed as:

$$-\frac{d\theta}{dt} = k'\theta + k_0. \qquad [A1]$$

After re-arrangement, and multiplication of both sides by $e^{k't}$, it transforms to:

$$e^{k't}\frac{d\theta}{dt} + ke^{k't}\theta = -k_0 e^{k't}. \qquad [A2]$$

Upon substitution, $ke^{k't} = \frac{de^{k't}}{dt}$ in Eq. A2, we get:

$$e^{k't}\frac{d\theta}{dt} + \frac{de^{k't}}{dt}\theta = -k_0 e^{k't}. \qquad [A3]$$

Applying the product rule, $(uv)' = u'v + v'u$, where, $u = \theta$ and $v = e^{k't}$, we get:

$$\frac{d}{dt}e^{k't}\theta = -k_0 e^{k't}. \qquad [A4]$$

Both sides of Eq. A4 can be integrated which leads to the solution with free constant C shown below:

$$e^{kt}\theta = -\frac{k_0}{k'}e^{k't} + C. \qquad [A5]$$

After solving for θ, we get

$$\theta = (e^{-k't}\cdot C) - \frac{k_0}{k'}. \qquad [A6]$$

From initial conditions we can evaluate the constant C. At t = 0, θ = 1, thus yielding $C = (1 + \frac{k_0}{k'})$. Therefore, "*oxygen-corrected first order rate equation*", is defined as:

$$\theta(t) = \left(1 + \frac{k_0}{k'}\right)e^{-k't} - \frac{k_0}{k'}. \qquad [A7]$$

Derivation of the OCP model using "oxygen-corrected first order rate equation".—When the UPD process represents a single energy state, and its electrosorption valence is equal to the oxidation state of metal ions in the solution, *Swathirajan and Bruckenstein* have developed isotherm (BS isotherm) describing the underpotential-coverage dependence as;[32]

$$\Delta E = \Delta E^0_{\theta\to 0} - \frac{RT}{mF}\left[\ln\left(\frac{\theta}{1-\theta}\right) + f\theta + g\theta^{3/2}\right]. \qquad [A8]$$

The RT/mF term for the case of Pb UPD ML has the value of 0.013 V at room temperature. In an ordinary experiment, one rather measures a potential E than the underpotential ΔE, where ΔE can be always expressed as $E\text{-}E_{m/m^+}$. Therefore ΔE can be substituted with E without changing the mathematical relation and its physical meaning. Combining above equation with the *"oxygen-corrected first order rate equation"*, Eq. A7, we get the final form of the equation used to model OCP transients from deposition experiments as:

$$E = E_{\theta\to 0} - 0.013\text{V}\left\{\ln\frac{\left(\left(1+\frac{k_0}{k'}\right)e^{(-k't)} - \frac{k_0}{k'}\right)}{\left(1+\frac{k_0}{k'} - \left(1+\frac{k_0}{k'}\right)e^{(-k't)}\right)} + f\left(\left(1+\frac{k_0}{k'}\right)e^{(-k't)} - \frac{k_0}{k'}\right) + g\left(\left(1+\frac{k_0}{k'}\right)e^{(-k't)} - \frac{k_0}{k'}\right)^{3/2}\right\}. \qquad [A9]$$

List of Symbols

C^{∞}_{Au}	Bulk concentration of gold ions
C^{is}_{Au}	Surface concentration of gold ions
$C^{\infty}_{HClO_4}$	Concentration of perchloric acid-supporting electrolyte
C^{∞}_{Pb}	Bulk concentration of lead ions
$C^{\infty}_{O_2}$	Bulk concentration of dissolved oxygen
D_{O_2}	Diffusion coefficient of oxygen molecule in solution
ΔE	Underpotential
ΔE_{EMF}	Electromotive force for galvanic displacement i.e electrochemical driving force for SLRR reaction.
$E_{\theta\to 0}$	Potential at which Pb UPD coverage tends to zero
e	Elementary charge
F	*Faraday's* constant
f	*Temkin* parameter
$\Delta G^{\#}$	Free energy of the activated complex
ΔG_{SLRR}	Free energy of the SLRR reaction
g	*Frumkin* parameter
k_0	Rate constant for the zero order reaction kinetics (Pb UPD ML oxidation via dissolved oxygen)
k_B	Boltzmann constant
k'	Rate constant for the first order reaction kinetics (Au deposition via SLRR of Pb UPD ML)
L	SLRR reaction order in terms of the depositing metal reactant (Au^{3+})
m	Stoichiometry coefficient for metal M, (oxidation state of metal M)
p	Stoichiometry coefficient for metal P, (oxidation state of metal P)
R	Universal gas constant
T	Absolute temperature

Greek

θ	Pb UPD ML coverage
Γ^{UPD}_{Pb}	Surface concentration of the full Pb UPD ML on Au(111)
ξ	Interface width
δ	Thickness of the diffusion layer
λ_D	Debye length
λ	Reorganization energy
σ	Standard deviation of the fit

References

1. S. R. Brankovic, J. X. Wang, and R. R. Adzic, *Surface Science*, **474**, L173 (2001).
2. K. Sasaki, J. X. Wang, H. Naohara, N. Marinkovic, K. More, H. Inada, and R. R. Adžić, *Electrochim. Acta* **55**, 2645 (2010).
3. A. Nilekar, Y. Xu, J. Zhang, M. Vukmirovic, K. Sasaki, and R. Adžić, M. Mavrikakis, *Top. Catal.* **46**, 276 (2007).
4. N. Dimitrov, *Electrochimica Acta*, **209**, 599 (2016).
5. S. R. Brankovic and G. Zangari in *Chapter 3: Electrochemical Surface Professes and Opportunities for Material Synthesis*, Electrochemical Engineering Across Scales: From Molecules to Processes, Editors: R. C. Alkire, P. N. Bartlett, and J. Lipkowski,

Advances in Electrochemical Science and Engineering, Vol. **15**, Willey-VCH (2015) p. 59.
6. M. B. Vukmirovic, S. T. Bliznakov, K. Sasaki, J. X. Wang, and R. R. Adžić, *The Electrochemical Society Interface*, **20**, 33 (2011).
7. Y. G. Kim, J. Y. Kim, D. Vairavapandian, and J. L. Stickney, *The Journal of Physical Chemistry B*, **110**, 17998 (2006).
8. C. Mitchell, M. Fayette, and N. Dimitrov, *Electrochimica Acta*, **85**, 450 (2012).
9. J. Nutariya, M. Fayette, N. Dimitrov, and N. Vasiljevic, *Electrochimica Acta*, **112**, 813 (2013).
10. S. R. Brankovic, N. Vasiljevic, and N. Dimitrov in *Chapter 27- Applications to Magnetic Recording and Microelectronic Technologies*, Modern Electroplating V, editors: M. Paunovic and M. Schlesinger, John Willey and Sons, Inc (2010), p. 573.
11. S.-E. Bae, D. Gokcen, P. Liu, P. Mohammadi, and S. R. Brankovic, *Electrocatalysis*, **3**, 203 (2012).
12. D. Gokcen, Q. Yuan, and S. R. Brankovic, *Journal of The Electrochemical Society*, **161**, D3051 (2014).
13. M. Fayette, Y. Liu, D. Bertrand, J. Nutariya, N. Vasiljevic, and N. Dimitrov, *Langmuir*, **27**, 5650 (2011).
14. L. T. Viyannalage, R. Vasilic, and N. Dimitrov, *Journal of Physical Chemistry C*, **111**, 4036 (2007).
15. J. Zhang, K. Sasaki, E. Sutter, and R. R. Adžić, *Science* **315**, 220 (2007).
16. R. Loukrakpam, Q. Yuan, V. Petkov, L. Gan, S. Rudi, R. Yang, Y. Huang, S. R. Brankovic, and P. Strasser, *Phys. Chem. Chem. Phys.*, **16**, 18866 (2014).
17. D. Gokcen, S.-E. Bae, and S. R. Brankovic, *Journal of the Electrochemical Society*, **157**, D582 (2010).
18. D. Gokcen, S.-E. Bae, and S. R. Brankovic, *Electrochimica Acta*, **56**, 5545 (2011).
19. K. Venkatraman, R. Gusley, L. Yu, Y. Dordi, and R. Akolkar, *Journal of The Electrochemical Society*, **163**, D3008 (2016).
20. R. Vasilic, N. Vasiljevic, and N. Dimitrov, *Journal of Electroanalytical Chemistry*, **580**, 203 (2005).
21. W. H. Press, B. P. Flannery, S. A. Teukolsky, and W. T. Vetterling, *Numerical Recipes – The Art of Scientific Computing*, Cambridge University Press, Cambridge, (1989) p.521.
22. R. R. Adžić in *Chapter 5-Recent Advances in the Kinetics of Oxygen Reduction*, Electrocatalysis, J. Lipkowski and P. N. Ross (Eds.), Wiley-VCH, New York, 1998, p. 197.
23. E. Bulut, *Reaction Kinetics of Metal Deposition by Surface Limited Redox Replacement of UPD Monolayer*, PhD Thesis, University of Houston, (2015).
24. L. Ke, *A Method of Light Reflectance Measurement*, *Master Thesis*, Tsinghua University, (1993) (see references therein).
25. A. Bewick and B. Thomas, *Journal of Electroanalytical Chemistry and Interfacial Electrochemistry*, **65**, 911 (1975).
26. A. Bewick and B. Thomas, *Journal of Electroanalytical Chemistry and Interfacial Electrochemistry*, **84**, 127 (1977).
27. D. M. Kolb and R. Kotz, *Surface Science*, **64**, 96 (1977).
28. D. M. Kolb and R. Kotz, *Surface Science*, **64**, 698 (1977).
29. R. Adžić, E. Yeager, and B. D. Cahan, *J Electrochem. Soc.: Electrochemical Science and Technology*, **121**, 474 (1974).
30. Y. Mo, Y. Gofer, E. Hwang, Z. Wang, and D. A. Scherson, *Journal of Electroanalytical Chemistry*, **409**, 87 (1996).
31. J. M. Smith, *Chemical Engineering Kinetics*, 2nd edition, Mc. Graw Hill, New York (1970), p. 47, p. 52.
32. S. Swathirajan and S. Bruckenstein, *Electrochimica Acta*, **28**, 865 (1983).
33. W. Schmickler, *Interfacial Electrochemistry*, Oxford University Press, New York (1996) p. 21.
34. S. Glasstone, K. J. Laidler, and H. Eyring, *The Theory of Rate Processes*, McGraw-Hill, New York, (1941).
35. R. A. Marcus, *Annu. Rev. Phys. Chem.* **15**, 155 (1964).
36. W. C. McC. Lewis, *J. Chem. Soc. (London)*, **113**, 471 (1918).
37. M. Polanyi, *Z. Electrochem.*, **26**, 50 (1920).
38. A. J. Bard and L. R. Faulkner, *Electrochemical Methods Fundamentals and Applications*, Wiley: New York, (1980) p. 87.
39. D. M. Kolb, *Journal of Solid State Electrochemistry*, **15**, 1391 (2011).
40. L. Pauling, *General Chemistry*, Dover Publications, New York (1970), p. 663.
41. P. Debye and E. Hückel, *Physikalische Zeitschrift*. **24**, 185 (1923).